Thermal Analysis of a Passenger-Loaded Vehicle in Severe Winter Conditions

G. Karimi, PhD **Syed R. Iqbal** **J. Richard Culham, PEng, PhD**

Received October 13, 2005; accepted June 8, 2007

In this paper, a thermophysical model of the dynamic interactions between an automobile driver and a heated seat is presented. The contacting body is considered to be made of three layers—core, skin, and clothing—while the seat consists of several layers of fabric materials. Experimentally measured load distributions are used to identify the distribution of local thermal resistance across the contact areas and to determine the spatial and temporal variation in the temperature of the seat and of the driver's skin and clothing. The model, which has the ability to predict the transient response of a driver in a highly nonuniform thermal environment, has been tested under simulated winter conditions. The good agreement between model predictions and experimental measurements suggests that such a model can be a useful predictive tool in the design of automobile heated seat systems. The experimentally measured local thermal sensations can be beneficial to the vehicular seat designers.

INTRODUCTION

Automobile cabin temperatures can drop to subzero levels during harsh winter conditions. Under such freezing conditions, an automobile driver could experience localized cooling as his/her exposed body surfaces (15% to 20%) make contact with the cold seat, back support, and steering wheel. Although the heating system within an automobile attempts to respond to the comfort needs of the driver, the thermal capacity of most cabin components limits the timely response of the heating system, resulting in driver discomfort for extended periods.

In the past three decades, automotive manufacturers have introduced heated seats in selected models to enhance drivers' thermal comfort particularly during the initial periods of driving. In these systems, heat is generated electrically in heating pads located underneath the seat cover and transferred through the seat to reduce the conduction heat losses from the driver's body in contact areas. This new feature has motivated interest in the development of more efficient driver's-seat heating systems to ensure driver thermal comfort under severe winter conditions.

The commonly used system evaluation procedure, which involves measuring the rise in compartment air temperatures at selected locations during the warm-up process, may not be adequate to assess a driver's thermal comfort because a significant amount of heat is exchanged in the contact areas. A more fundamentally sound, albeit expensive and time consuming, procedure is to use test subjects to evaluate thermal comfort under simulated winter driving conditions. In this procedure, teams of test subjects sit on fully equipped seats while they subjectively evaluate thermal sensations associated with the applied conditions. The test subjects must account for variations in local and overall thermal sensations produced by nonuniform thermal conditions.

The body of literature on the study of heat exchange between an automobile seat and its occupant is very limited. This is mainly due to the presence of a complicated thermal resistance

G. Karimi is an assistant professor in the Department of Chemical and Petroleum Engineering, Shiraz University, Shiraz, Iran. **Syed R. Iqbal** is an advanced specialist with W.E.T. Automotive Systems Ltd., Windsor, ON, Canada. **J. Richard Culham** is a professor in the Department of Mechanical Engineering, University of Waterloo, Waterloo, ON, Canada.

network resulting from the load distribution in contact areas. Burch et al. (1992a, 1992b) developed a mathematical model of thermal interactions between a driver and the interior environment of an automobile for which good agreement was reported between model predictions and jury data. This model was later extended by Karimi et al. (2002, 2003) to predict the transient response of a driver in a highly nonuniform thermal environment. Constant thermal resistances were considered in the seat backrest and cushion areas to predict time variations of the seat and occupant temperatures. Relatively good agreement was found between the model predictions and experimental data using test subjects. Chan et al. (2004) performed steady-state thermal-mechanical simulations using I-DEAS 10 and the TMG package to study the effect of occupant load on the temperature distributions in a typical vehicle seat over a wide range of heat input levels.

This paper presents a comprehensive physical model for a heated seat interacting with an average driver under severe winter conditions. A systematic approach is taken to determine the network of thermal contact resistances at the occupant-seat interface. Three-dimensional physical models are developed to simulate temperature variations in the seat and the contacting body for a heated seat. Ergonomic studies are performed to evaluate a heated seat's performance in bringing thermal comfort to an automobile passenger under simulated winter conditions and to validate the accuracy and reliability of the occupant-seat physical models.

SEAT MODEL

A schematic of the heated seat under study is shown in Figure 1. The vehicle seat consists of five layers. Polyurethane foam is used to form the basic seat structural features and to provide cushioning for the occupant. The foam is carved out to accommodate a heating pad and a highly porous spacer material (Muller™) for possible seat ventilation. The heating pad (also called Carbotex™) is made of a thin nylon fabric with carbon fibers sewn on in a regular pattern. The Carbotex™ and Muller™ spacer cover the middle section of the seat cushion and the backrest

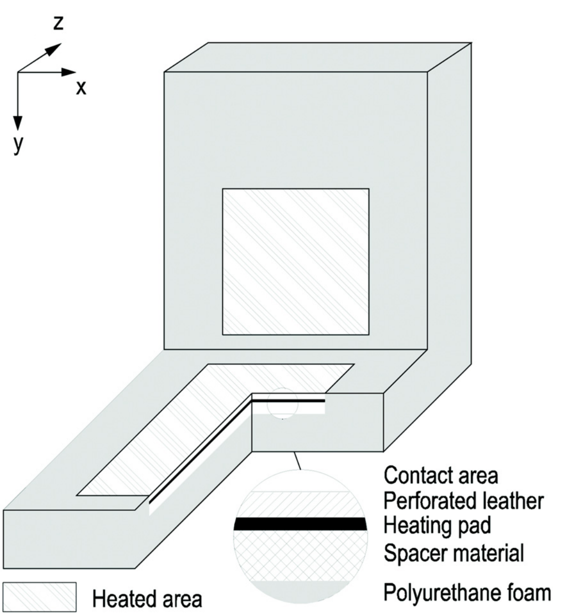

Figure 1. Schematic of a typical heated seat.

where maximum contact exists with the driver, as indicated in Figures 1 and 4. The other side of the seat is covered by a layer of leather. When activated, electric current from the vehicle battery passes through the carbon fibers and generates heat uniformly in the Carbotex^{TM} that is then conducted through the seat. The heat transfer in the seat is three-dimensional in general; however, the thermal resistance of the Muller^{TM} spacer and the foam are so large that a significant portion of the heat is transferred toward the seat surface in contact with the occupant. Neglecting the natural convection in the porous material, the seat governing equation can be expressed as

$$\rho c \frac{\partial T}{\partial t} = k\nabla^2 T + S \ , \tag{1}$$

where the seat local temperature, T, varies with spatial coordinates (x, y and z) and time, t. The thermophysical properties ρ, c, and k are the material density, specific heat, and thermal conductivity, respectively. The source term, S, is the heat generation per unit volume of the heating pad and is zero for unheated parts of the seat.

In practice, the seat materials and the fabric used in the seat manufacturing have small thermal conductivities. As a result, the thermal resistances in the spanwise directions are significant and the majority of heat is transferred perpendicular to the seat surface. Hence, the seat curvatures can be neglected and a block model as shown in Figure 1 can be considered for the analysis. To facilitate the computations, a symmetric condition is also assumed to limit the computational domain to half of the seat.

Equation 1 is subject to the following initial and boundary conditions:

$$T|_{t=0} = T_i \tag{2}$$

and

$$\left.\frac{\partial T}{\partial x}\right|_{x=0} = 0 \ \text{ symmetric seat} \tag{3}$$

$$Q = \begin{cases} \Delta T / R_c & \text{covered/contact area} \\ \Delta T / R_{amb} & \text{uncovered area} \end{cases} \tag{4}$$

where T_{amb} is the initial temperature of the seat.

Heat transfer from the seat surface occurs by a combination of convection and radiation in regions where the seat is directly exposed to the ambient air and by conduction in the contact areas with the seat occupant. The thermal resistance due to the convection and radiation in the uncovered areas (including side surfaces), R_{amb}, can be related to an effective heat transfer coefficient, h_{eff}, as:

$$R_{amb} = \frac{1}{h_{eff} A} \tag{5}$$

$$h_{eff} = h_{conv} + h_{rad} = C\left(\frac{T - T_{amb}}{\mathrm{R}}\right) + \varepsilon\sigma(T^2 + T_{amb}^2)(T - T_{amb}) \ , \tag{6}$$

where T_{amb} is the ambient temperature, R is a characteristic length, ε is the surface emissivity, and σ is the Stefan-Boltzmann constant. The constant C is 1.42 and 1.32 for horizontal and vertical surfaces, respectively (Holman 1997). The thermal contact resistance on the seat surface is expected to change with the passenger load and is determined experimentally through a postural pressure study and heat flux measurement, as discussed in the following sections.

EXPERIMENTS

Participant-Based Postural Study

The objective of the postural study is to obtain a representative occupant imprint and load distribution on the vehicle seat. The load distributions are essential to establishing a thermal resistance network in the contact areas. The pressure distributions are measured using two Tekscan^{TM} pressure mats, which were secured on the seat cushion and backrest. Each pressure mat is 48 cm wide and 42 cm long and is equipped with 2016 load cells to precisely measure the load distributions. Ten participants were chosen to yield a representative distribution on gender, age, and body types. Each participant was informed of the nature of the study and was instructed to assume a neutral seating posture. The total seating period was five minutes for each participant, and a time-averaged pressure distribution was taken.

Figures 2a and 2b display the averaged pressure distributions on the seat backrest and cushion, respectively. The load distributions due to the male and female occupants are very similar in shape. The maximum pressures are about 2.6 kPa on the seat backrest and 6.5 kPa on the seat cushion, corresponding to the shoulder area and pelvic region, respectively. Pressure distributions are slightly asymmetric, with the heavier loads covering a larger area in the right side of the body. The discontinuities in the pressure distributions along the dashed lines on the cushion side are due to the elevation change in the cushion side areas. The discontinuities on the seat backrest along the dashed line are insignificant. With the load distribution known, it is possible to determine the thermal resistances at the contact areas.

Thermal Resistance Network

Transfer of heat between the seat surface and skin is quite complicated, involving internal convection and radiation processes in the clothing pores and the conduction through the cloth itself. Generally, a heated manikin is used to accurately measure the effective thermal conductivity of different clothing ensembles. Energy exchange between a driver's body and the automobile seat can be estimated through a thermal resistance network extending from the driver's body core to the skin, clothing, and seat surface. The thermal contact resistance due to the clothing is expected to change with the applied load, particularly if the thermal conductivity of the clothing differs significantly from that of the air gaps. A series of experiments based on ASTM D5470-01 (ASTM 2005) was devised to measure the effective thermal resistance of some clothing materials as a function of load. Denim was chosen to represent the driver's clothing. Experiments were conducted on 1 mm thick denim samples using an apparatus shown in Figure 3. Thermal resistances were measured by determining the temperature drop across the specimens for pre-set heat flow rates. The applied load ranged from 1 to 100 kPa. The details of the test rig and experimental procedure can be found in Culham et al. (2002). The experimental data displayed that a linear relationship exists between the thermal resistance and the applied load as given below:

$$R_c = 10.876 - 0.031P \tag{7}$$

where P is in kPa. As expected, denim resistance decreases with the applied load; however, this dependency is very weak. The maximum reduction in the thermal resistance for an average

(a)

(b)

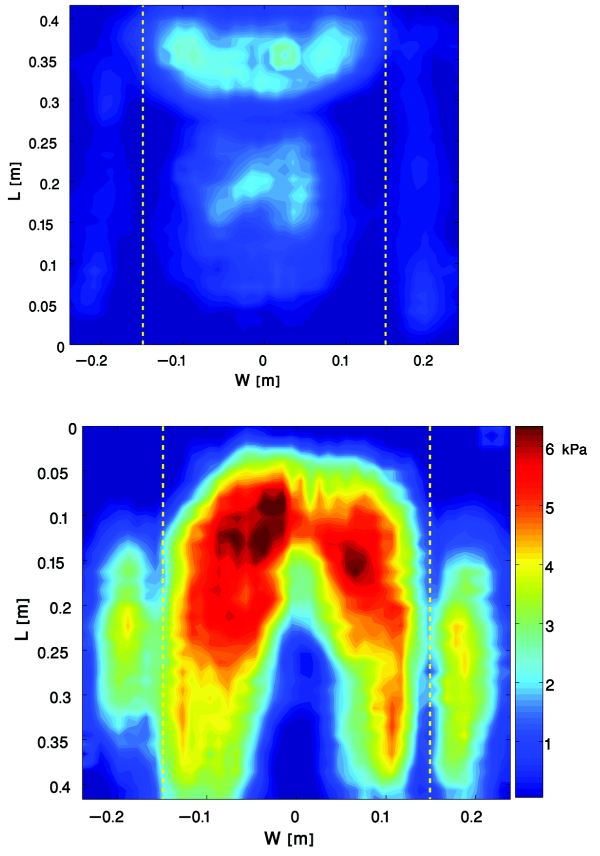

Figure 2. Average pressure distribution on the seat surface (a) backrest and (b) cushion side.

driver's load is less than 2%. This implies that the heat transfer in the contact area is almost uniform.

Temperature Measurements

Experimentally measured seat-occupant thermal interactions can be used to validate the accuracy and reliability of the physical models. In this work, a set of experiments was conducted to investigate the transient heat transfer between the seat and an average driver. A total of 26 individuals, half of them male and half female, with different ages, weights, and body types were engaged to undergo experiments for a period of two and a half hours. The program of measurements was carried out in a large windowless room 6 m wide and 8 m long with a ceiling height of 2.8 m. Experiments were performed during the month of August, so all subjects were clothed in cotton shirts and shorts or trousers and sandals. Pilot experiments were conducted on the first six subjects to determine the optimum experimental conditions. The room temperature and relative humidity were maintained constant at 22.5°C and 55%, respectively, by a central air-conditioning system. Although the type of the participant's clothing and room temperature did not represent realistic winter conditions, the experimental results can still be utilized for model validation and the seat performance can be evaluated.

The participants were first instructed regarding the purpose of the study and the experimental procedure. Then, their weights and heights were measured and their general information, such as age, body attributes, and general thermal comfort, were collected. The participants' skin temperatures were measured using eight thermistors (9.5 mm in diameter) placed at different body locations, four on the back and four on the thigh, as illustrated in Figure 4. In addition, nine type T thermocouples were placed on the seat cushion and the backrest at the contact areas to monitor the seat surface temperatures during each test.

The heating tests consisted of two experiments. The seat was cooled down to about –4°C by covering it with frozen ice packs. For each experiment, a thermal blanket was used to cover the

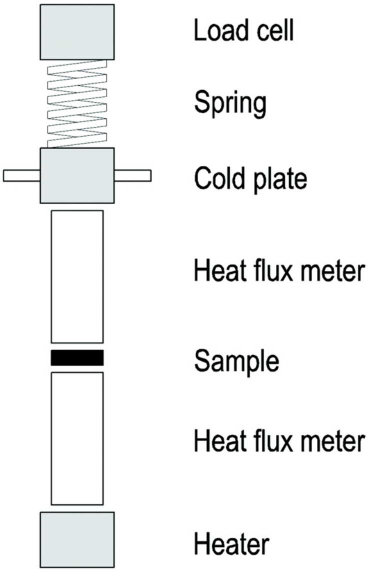

Figure 3. Thermal resistance measuring apparatus.

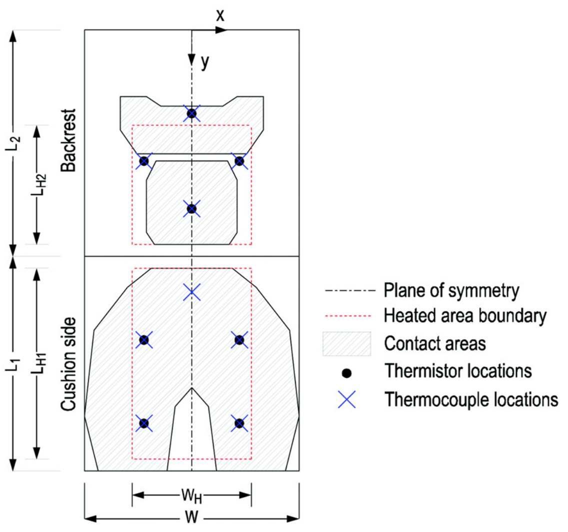

Figure 4. The approximate map of the body/cloth in contact with the seat and the measuring thermistors and thermocouples.

seat for a period of about 20 minutes to minimize the heat loss and to ensure a uniform temperature distribution with a reasonable penetration depth. Also, during the seat preparation the seat surface temperatures were monitored to ensure temperature level and uniformity. For each heating test, subjects were asked to stand calmly close to the seats for about 10 minutes. This period was necessary for the skin temperatures to achieve thermal equilibrium. The seat covers as well as the ice packs were then removed and the subjects were asked to immediately sit on the seats. Heating tests were conducted with and without activating the seat heater. Subjects were allowed to perform quiet activities such as reading and watching movies during the tests. The participant's skin temperature, the seat surface temperature, and the ambient temperature were collected and monitored using a data acquisition system. In addition, information on local thermal sensations was collected using a questionnaire. Subjects were asked to rank their thermal sensations at the back and cushion areas. The ranking was conducted in two-minute intervals during the tests. When giving partial thermal sensation, the subjects were instructed to disregard as much as possible sensations at other places on their bodies. Table 1 lists the statistics of the 20 subjects participating in the main study and the seat initial conditions.

SOLUTION METHOD

A finite volume scheme with variable cell spacing was developed to discretize Equation 1. The grid density is increased in the heated areas of the seat to capture detailed temperature distributions. An alternating direction implicit (ADI) was used to convert the original set of algebraic equations into tridiagonal matrices, which were then solved using a Thomas algorithm.

Thermal interaction between the seat and the driver's body at contact areas (Equation 4) was determined as follows. A pressure threshold (e.g., 0.2 kPa) was defined to identify the contact areas. The contacting body (skin and clothing) was divided into control volumes extending from the seat surface toward the body core. The core temperature was considered to be fixed at 37°C during the simulations, which is consistent with the numerical results from a previous study (Karimi et al. 2002). The room's average temperature was taken as ambient and wall surface temperature. A total of 81 W of heat was generated in the heating pads within the seat, which is then transferred to the contacting areas, dissipated to the ambient, or accumulated in the seat. All simulations were performed for a period of ten minutes, identical to the duration of the experiments. A time interval of ten seconds was chosen in all simulations. Table 2 lists the specifications of the

Table 1. Experimental Statistics

	Average	STD
Participants		
Age (year)	27.5	8.2
Height (m)	1.73	10.1
Weight (kg)	75.0	22.3
Initial Skin Temperatures (°C)		
Thigh Area	32.6	0.3
Back Area	33.1	0.8
Seat		
Initial Seat Temperatures (°C)		
Cushion	–4.0	1.1
Backrest	–0.1	1.5

Table 2. Parameters and Properties Used in the Seat Simulations

Seat Geometry (Figure 4)		Seat Materials	δ, mm	ρ, kg/m³	c, J/kg·°C	k, W/m·°C)
W	0.46 m	Leather	1	556	1300	0.08
L_1	0.42 m	Carbotex™	0.5	500	1515	0.10
L_2	0.50 m	Muller™	10	50	800	0.04
W_H	0.26 m	Foam	100	70	1340	0.03
L_{H1}	0.40 m	Leather	1	556	1300	0.08
L_{H2}	0.21 m					
Seat Heater		**Contact Materials**	**δ, mm**	**ρ, kg/m³**	**c, J/kg·°C**	**k, W/m·°C)**
V	13.1 V	Denim	1	80	1300	0.06
I	6.0 A	Skin	10	900	3000	0.40
Controller Setpoints						
High	55°C					
Low	53°C					

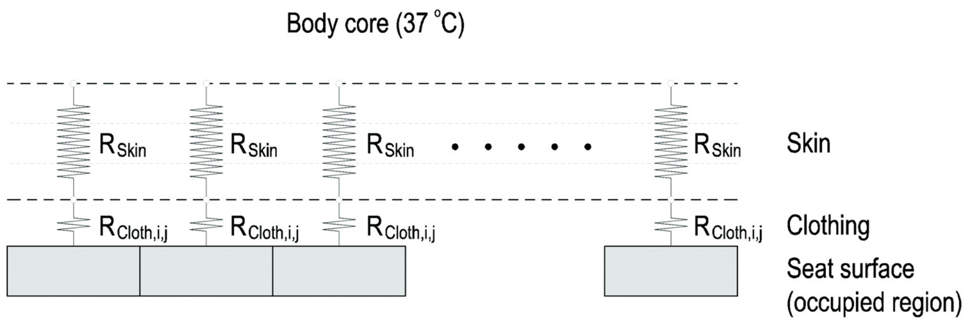

Figure 5. Schematic for the occupant-seat thermal resistance network.

vehicle seat under study. The physical properties of the seat materials and the contacting human body model are also given in the table.

RESULTS AND DISCUSSION

The heat transfer potentials of the seat are determined for the seat surface. Effective heat transfer coefficients on the seat surface, $h_{eff}(x,y)$, are calculated based on the local thermal resistances. Equations 6 and 7 are used to calculate h_{amb} in the unoccupied region and h_c in the contact area, respectively.

Figure 6 displays variations of h_{eff} on the seat cushion and backrest at the end of the simulation period (i.e., ten minutes). Careful examination of this figure indicates that there exist two distinct heat transfer regions on the seat surface: the occupied regions with an effective heat transfer coefficient of about 142 W/(m^2·°C), which is independent of the time, and the unoccupied areas with the effective heat transfer coefficient varying between 8 and 12 W/(m^2·°C) as the seat local temperatures vary with time.

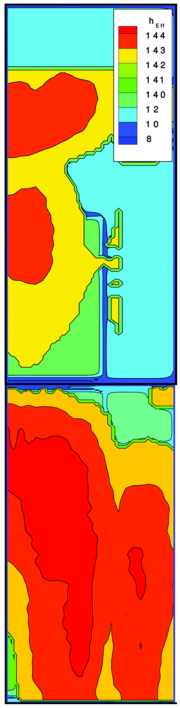

Figure 6. Distribution of the effective heat transfer coefficients on the surfaces of the seat cushion and backrest after ten minutes.

Figure 7 shows the simulated temperature distributions on the seat surface for different time intervals. Figure 7a shows the temperature response in the time interval right after the seat is occupied. The seat surface temperature in the occupied region rises from approximately 0°C to 15°C in roughly 10 seconds. This is due to the large effective heat transfer coefficient and the higher temperature of the occupant's clothing in contact with the seat. The temperature of the unoccupied areas, on the other hand, does not change significantly as the seat is exchanging heat with the surroundings with smaller temperature differences and through larger thermal resistances. As time passes, more heat is transferred into the seat surface, partly from the contacting body and partly due to the conduction of heat from the heating pad toward the seat surface. As a result, the seat surface temperature increases with time. Figures 7b to 7d clearly show the conduction of the heat in the heated areas. The interesting feature of Figure 7d is that the seat surface temperature on the heated regions in contact with the body cannot exceed a certain limit, as the body core behaves like a heat sink of infinite thermal capacity (the core temperature is constant at 37°C). On the other hand, if the body is not contacting the heated areas, the temperature can attain higher values, but it is limited by the seat temperature controller and the ambient conditions.

Figure 8 shows the corresponding temperature distributions for the occupant's skin in contact with the seat cushion and backrest as a function of time. As shown in Figure 7a, the skin temperature drops right after it contacts the cold seat. Although the temperature drops on the cushion and backrest areas are almost the same, the skin in contact with the seat backrest shows a higher temperature after 10 s. This is due to the higher initial skin temperature measured for the majority of participants in the ergonomic study. The skin temperature continues to decrease for a

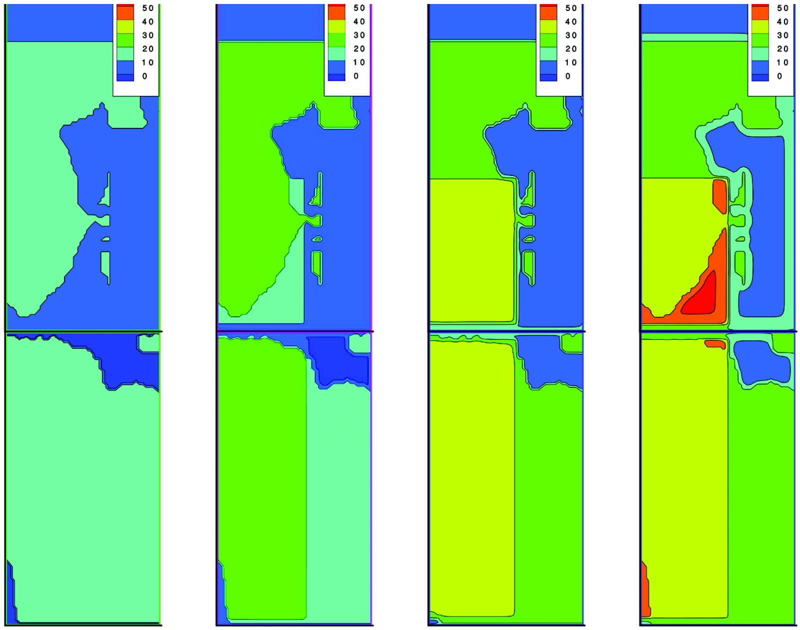

(a) t = 10 s (b) t = 1 min (c) t = 4 min (d) t = 10 min

Figure 7. Time variations of temperature distribution on the seat surface (heated).

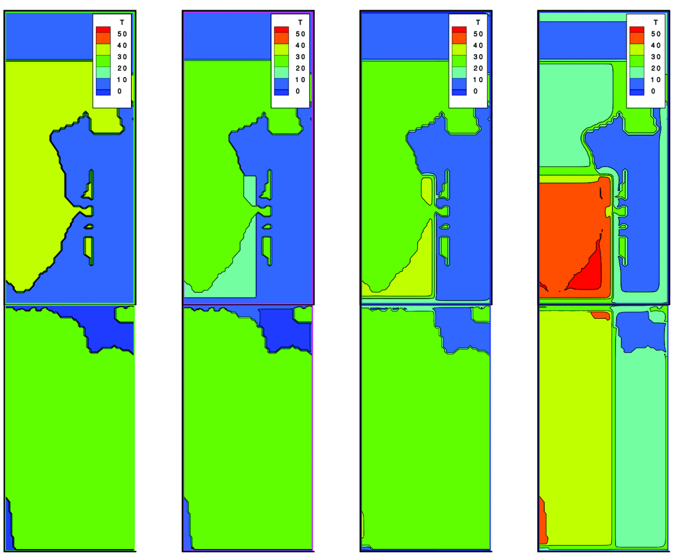

(a) t = 10 s (b) t = 1 min (c) t = 4 min (d) t = 10 min

Figure 8. Time variations of skin temperature distribution contacting with the heated seat.

period of 1 min and increases afterward as heat is conducted from the heated surface and the body core to the skin. Figure 8d clearly shows the effectiveness of the seat heater.

Figure 9 compares the seat and skin averaged temperatures predicted by the model with the corresponding measured participant-based data. The experimentally measured thermal sensations reported by the subjects as a function of time are also included in this figure. The results for both heated and unheated seats are presented. Figures 9a and 9b clearly show the sudden increase in the seat surface temperatures as the seat is brought in contact with the occupant. The initial rate of seat temperature rise is identical for both heated and unheated seats. This is because it takes some time before heat can penetrate through the relatively large thermal resistance of the perforated leather and reach the contacting body. As time elapses, the effect of the seat heater can be felt on the surface, resulting in a higher surface temperature for the heated seat. The rate of temperature increase is gradually diminished as the temperature gradients subside and a relative steady-state condition prevails at the end of the 10 min period. The present model is able to predict experimental data with a very good accuracy. The average errors are listed in Table 3.

Figures 9c and 9d display the variations of the skin temperatures in contact with the seat cushion and backrest, respectively. As expected, the skin temperature drops initially for both areas as the skin contacts with the cold seat. The rate and the magnitude of the temperature drop in the seat cushion and backrest is almost the same due to similar thermal resistance in the two regions. The temperature drops stop roughly after 1 min, and the skin temperature rises afterward. For a heated seat, heat is transferred from the body core and the heating pad resulting in quick skin temperature recovery. For an unheated seat, the rate of heat loss from the skin to the seat decreases with time due to the diminishing temperature gradient. However, the heat is still is transferred to the skin from the higher-temperature body core. The net effect will be a sluggish rise in the skin temperature. The present model will predict the trend in the skin temperature variations with time within a 5% error, as indicated in Table 3.

Figures 9e and 9f show participants' thermal sensations reported for the cushion and backrest areas as a function of time. In the present study, Fanger's thermal comfort scale was used to evaluate thermal sensations (Fanger 1970). This scale uses seven distinct numbers from –3 to +3 corresponding to very cold, cold, cool, neutral, warm, hot, and very hot. Participants were instructed to rate 0 for their thermally neutral sensations. As shown in the figures, participants reported, on average, cool-to-cold sensations in the seat cushion and backrest areas at the moment they sat on the seat. With the unheated seats, it took about ten minutes for the participants to reach thermal neutrality at contact areas. On the other hand, when the heating system was activated, local thermal sensations increased quickly and the participants felt warm after about three to four minutes. If the heating system is not shut down after this period, participants will feel localized heating at the contact areas with the seat, as shown in the figure. Again, the difference in thermal sensation ratings at the cushion and the backrest are due to different thermal capacities and thermal resistances from the skin to the seat in contacted areas.

The experimental data in Figures 9c and 9d clearly show that a comfortable local thermal sensation can be re-established before skin temperature has been restored to initial normal condition. On the other hand, that is the magnitude of the heat flow to or from the skin and *not* the skin temperature, which determines the thermal sensation. To address this issue, heat flow rates are calculated based on the measured temperature differences between the seat surface and the skin and the effective heat transfer coefficients at the time intervals for which the thermal sensation data are available. Figures 10a and 10b show the measured thermal sensations as a function of the instantaneous heat flow to the skin for cushion and backrest areas, respectively. The results indicate an exponential like variation of thermal sensations as a function of heat flux from the skin, which is in agreement with the correlation proposed by Fanger (1970). However, the experimental data for the cushion side display a larger slope than those of the backrest area. Further, the average thermal sensation reported in the backrest area is slightly positive at zero heat flux. Therefore, the experimental data for the cushion side seems to be more reliable. This is probably due to the fact that it was very difficult for the participants to interrupt their body contact with the seat in the cushion area, while the contact with the backrest could be interrupted from time to time during the course of the ergonomic tests.

SUMMARY AND CONCLUSIONS

A transient physical model was developed to simulate the thermal interactions between an automobile driver, the cabin environment, and a heated seat. The model uses the measured load

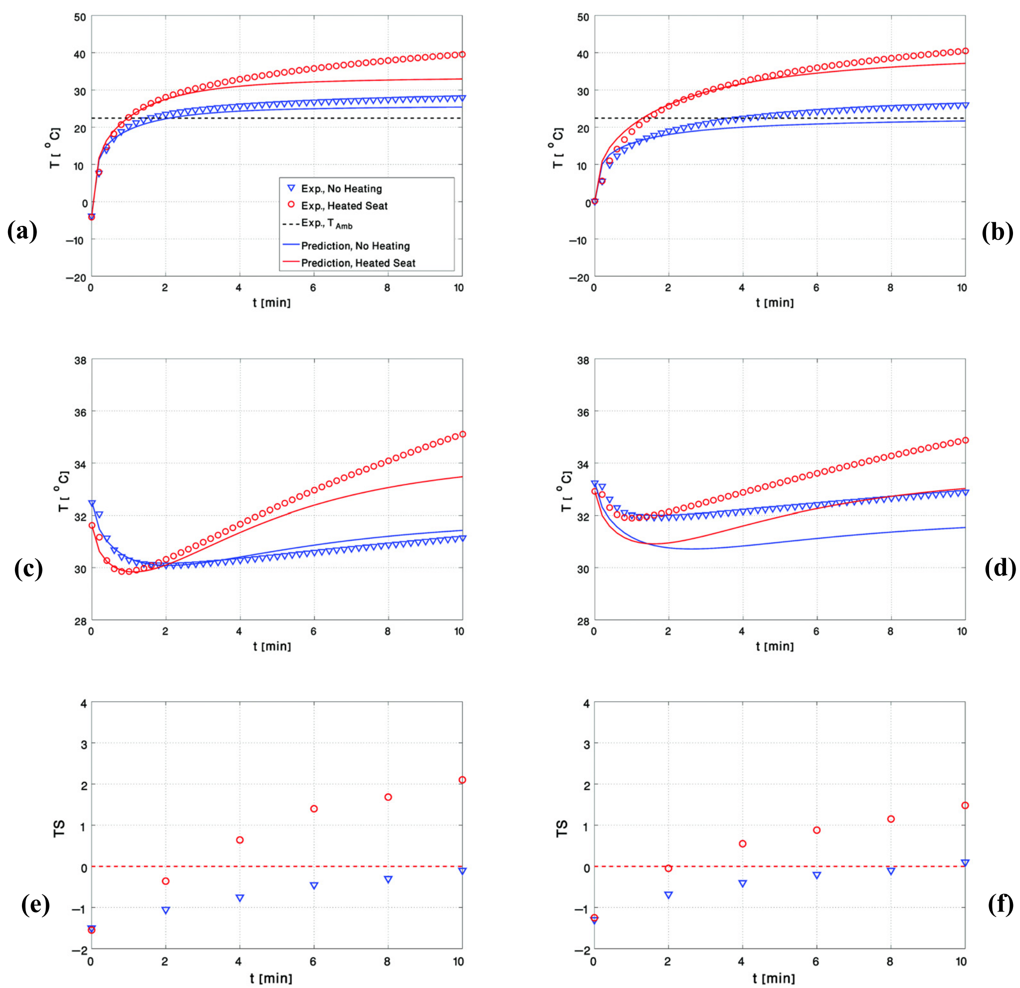

Figure 9. Comparison of the seat and skin averaged temperatures measured and simulated as a function of time for (a) seat temperature, cushion side; (b) seat temperature, backrest; (c) skin temperature, cushion side; (d) skin temperature, backrest. Time variations of local thermal sensations for (e) thermal sensation, cushion side; and (f) thermal sensation, backrest.

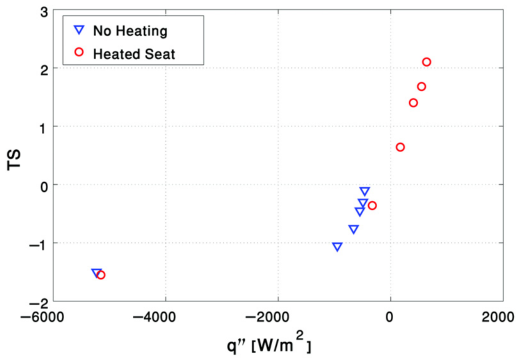

(a)

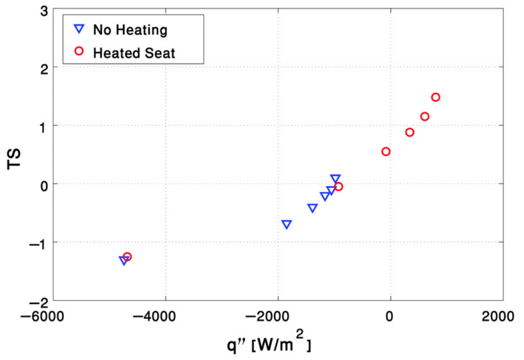

(b)

Figure 10. Occupants' thermal sensations versus body heat flux (a) cushion side and (b) backrest area.

Table 3. Computational Error for the Seat Surface and Skin Temperatures

Segment	Average Error, %	
	Unheated Seat	**Heated Seat**
Seat Surface		
Cushion Side	5.0	6.6
Backrest	7.8	–0.5
Skin		
Cushion Side	–0.5	1.8
Backrest	3.7	3.9

distribution in the driver's-seat contacting areas to develop a thermal resistance network and to determine the rate of heat transfer. From the experimental measurements and the simulation results, it can be concluded that the effect of the driver's weight on the thermal resistances in the driver's-seat contact areas is insignificant. This causes a relatively uniform temperature to be developed on the driver's skin in contacted areas. Hence, it can be concluded that designing a nonuniform heating pattern on the seat heating pads seems to be undesirable. The data from experiments including human subjects clearly indicate a strong dependence between the direction and the magnitude of the heat flow and local thermal sensations in contact areas.

ACKNOWLEDGMENTS

The authors would like to acknowledge the financial support of Materials and Manufacturing Ontario (MMO), the Natural Sciences and Engineering Research Council of Canada (NSERC), and W.E.T. Automotive Systems Ltd.

NOMENCLATURE

A	=	heat transfer area, m^2	Q	=	heat transfer rate, W
c	=	specific heat, J/kg·°C	q''	=	heat flux, W/m^2
C	=	constant	R	=	thermal resistance, °C/W
h	=	heat transfer coefficient, $W/m^2{\cdot}°C$	S	=	heat generation rate, W/m^3
I	=	current, A	t	=	time, s
k	=	thermal conductivity, W/m·°C	T	=	temperature, °C
L	=	length, m	V	=	voltage, V
R	=	characteristic length, m	W	=	width, m
P	=	loading pressure, kPa	x, y, z	=	spatial coordinates, m

Greek Letters

δ	=	thickness, mm	σ	=	Stefan-Boltzmann constant, $\equiv 5.67 \times 10^{-8}$ $W/m^2{\cdot}K^4$
Δ	=	difference			
ε	=	surface emissivity	ρ	=	density, kg/m^3

Subscripts

I	=	initial condition	eff	=	effective
amb	=	ambient	H, H_1, H_2	=	heated areas
c	=	contact			
$conv$	=	convection	rad	=	radiation

REFERENCES

ASTM. 2005. ASTM D 5470-01, Standard test method for thermal transmission properties of thin thermally conductive solid electrical insulation materials. *ANSI Book of Standards*, 10.02.

Burch, S.D., S. Ramadhyani, and J.T. Pearson. 1992a. Experimental study of passenger thermal comfort in an automobile under severe winter conditions. *ASHRAE Transactions* 97:239–46.

Burch, S.D., S. Ramadhyani, and J.T. Pearson. 1992b. Analysis of passenger thermal comfort in an automobile under severe winter conditions. *ASHRAE Transactions* 97:247–57.

Chan, E.C., G. Karimi, D. Rose, and J.R. Culham. 2004. Mechanical-thermal simulation of passenger-loaded vehicle seat in severe winter conditions. Paper no. 2004-01-1507. *SAE 2004 World Congress, Detroit, MI, March 8–11*.

Culham, J.R., P.M. Teertstra, I. Savija, and M.M. Yovanovich. 2002. Design, assembly and commissioning of a test apparatus for characterizing thermal interface materials. *8th Intersociety Conference on Thermal and Thermomechanical Phenomena in Electronic Systems, San Diego, CA, May 29–June 1*.

Fanger, P.O. 1970. *Thermal Comfort Analysis and Applications in Environmental Engineering*. New York: McGraw-Hill.

Holman, J.P. 1997. *Heat Transfer*, 8th ed. New York: McGraw-Hill.

Karimi, G., E.C. Chan, J.R. Culham, I. Linjacki, and L. Brennan. 2003. Thermal comfort analysis of an automobile driver with heated and ventilated seat. Paper no. 2002-01-0222. *SAE 2002 World Congress, Detroit, MI, March 4–7*.

Karimi, G., E.C. Chan, and J.R. Culham. 2003. Experimental study and thermal modeling of an automobile driver with heated and ventilated seat. *Journal of Passenger Cars–Electronic and Electrical Systems, SAE Transactions*, pp. 682–92.